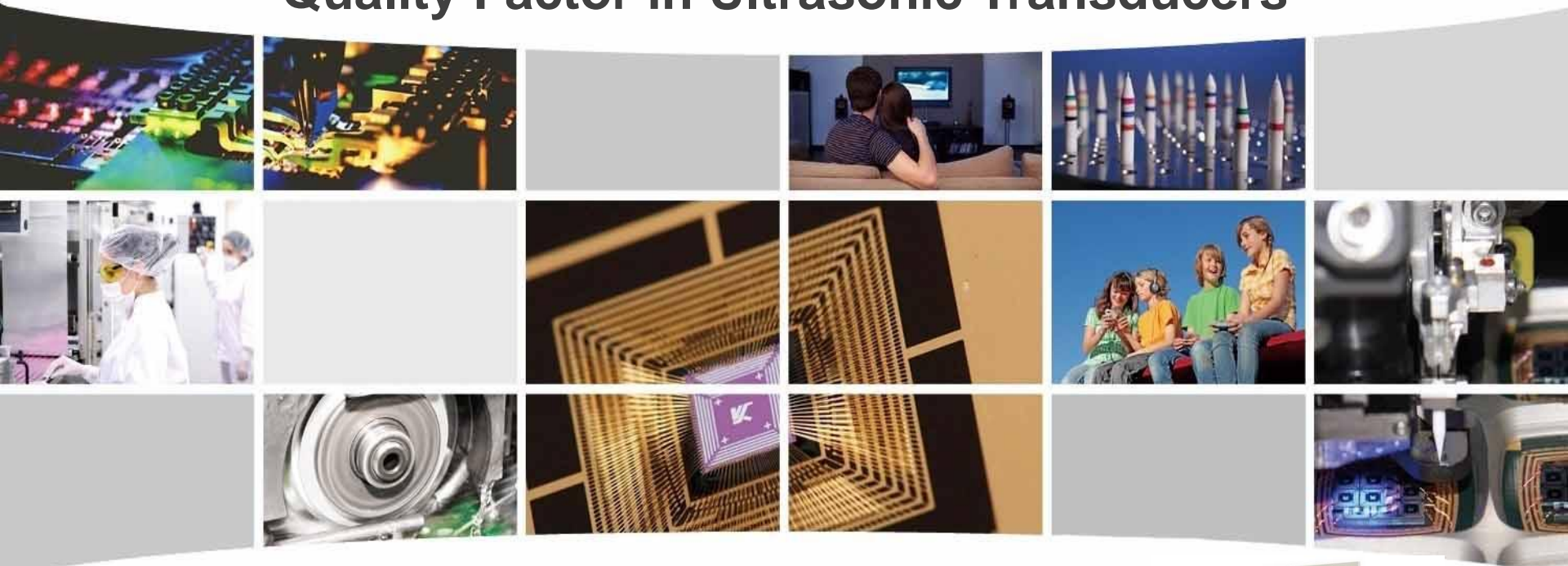


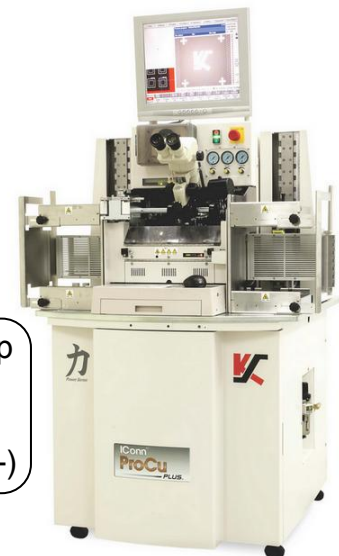
Predicting the Displacement Gain from the Mechanical Quality Factor in Ultrasonic Transducers



Dominick A. DeAngelis



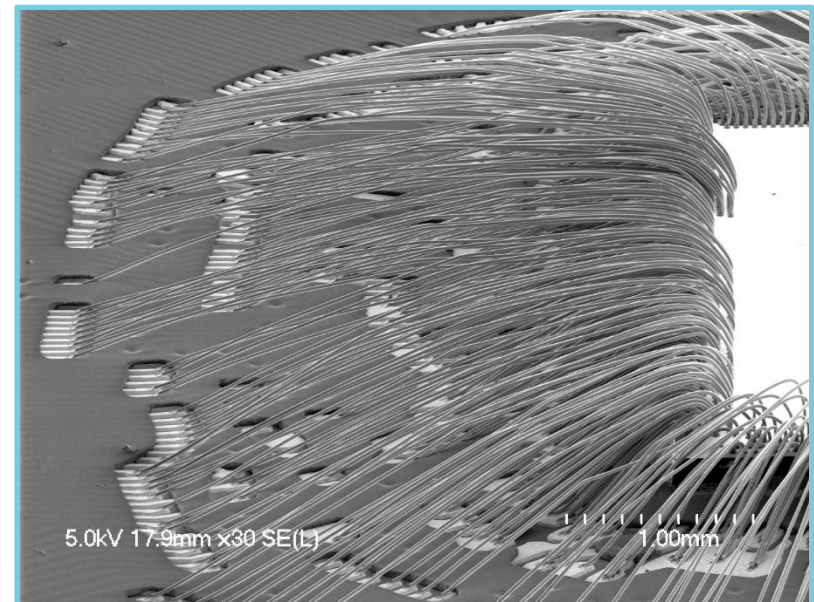
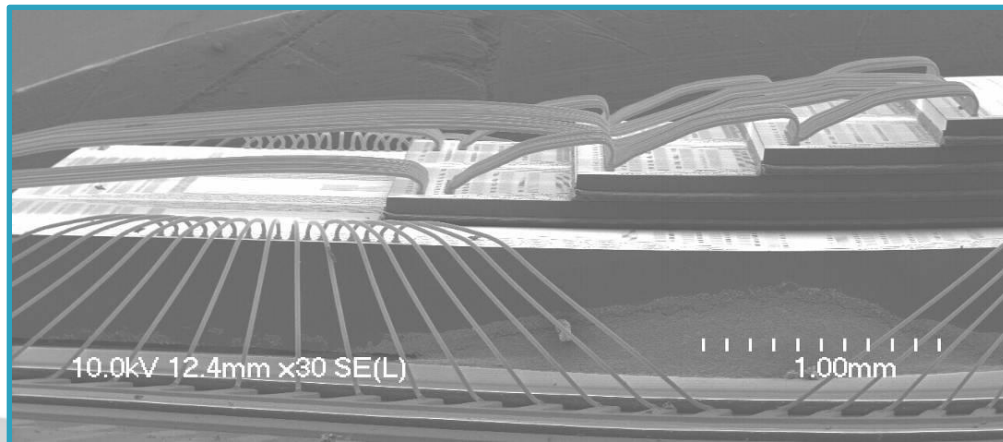
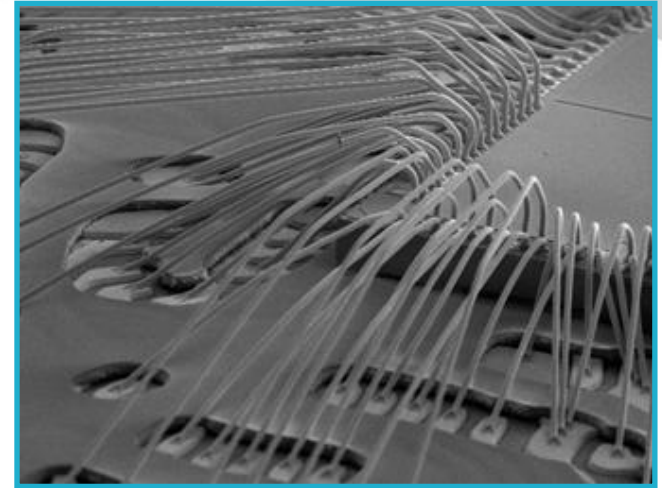
K&S's Flagship
Wirebonding
Machine
(IConn ProCu+)



44th UIA Symposium, Washington, DC, USA 20-Apr-15

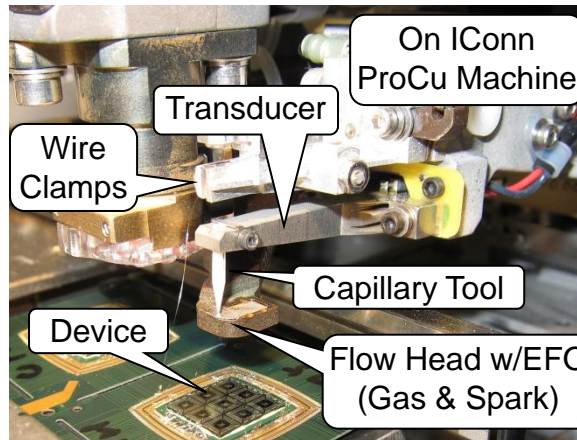
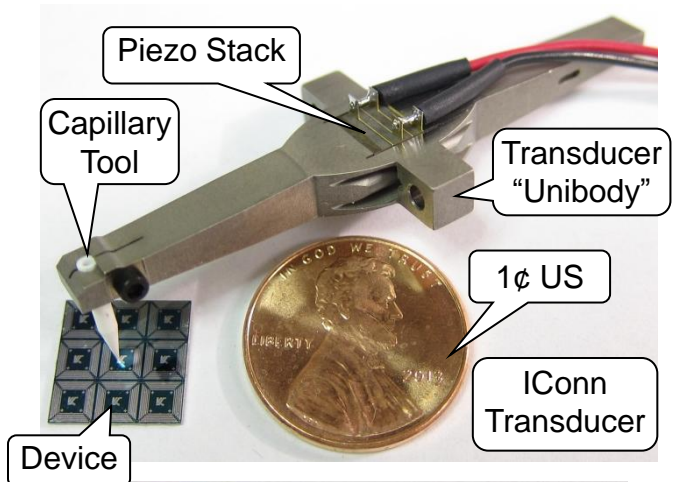
Outline

- ❖ Specific Transducer Application
- ❖ Motivation for the Research
- ❖ Definition of Mechanical Quality Factor (Q_m)
- ❖ Definition of Displacement Gain
- ❖ Methods for Measuring Q_m
- ❖ Equivalent Circuit Analysis for δ (Log Dec)
- ❖ Numerical Data Analysis for δ (Log Dec)
- ❖ Displacement Gain Vs. Q_m Derivation
- ❖ Experimental Results
- ❖ Conclusions
- ❖ Questions?

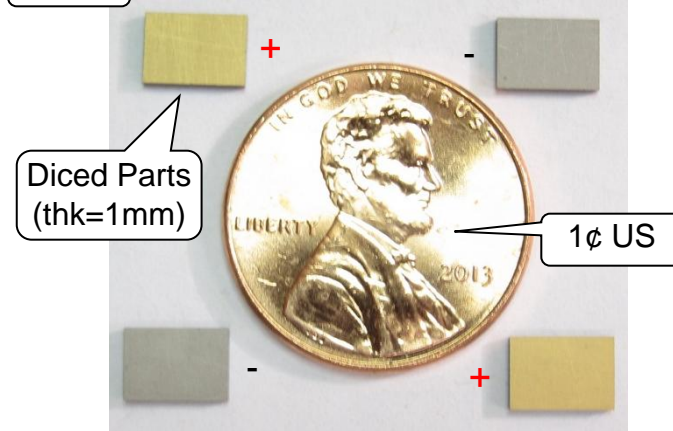


Specific Transducer Application

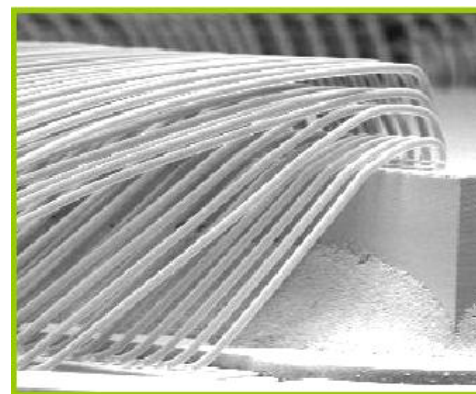
- ❖ K&S is the leading MFG of semiconductor wire bonding equipment
- ❖ The transducer delivers energy to a capillary tool for welding tiny wires
- ❖ Patented single piece “Unibody” design is ideal for research studies
- ❖ Portability across 100’s of machines required for same customer device



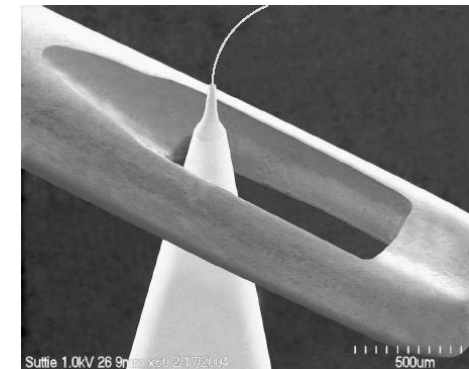
Transducer Specs
 500 mA Max Current
 50/120 kHz Operating Modes
 30 Ohm Typical Impedance
 Operation 40 Bonds/Sec
 Bond Duration ~10 mSec
 PZT8 Piezoceramics (4X)



PZT8 Piezoceramics



Actual Wire Bonds From Multi-Tier Package



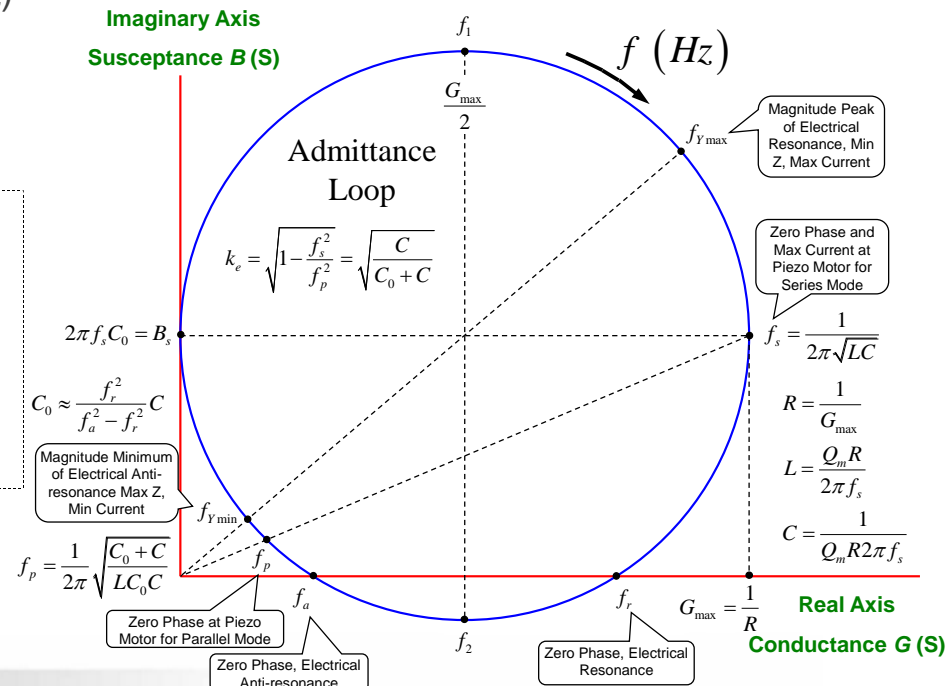
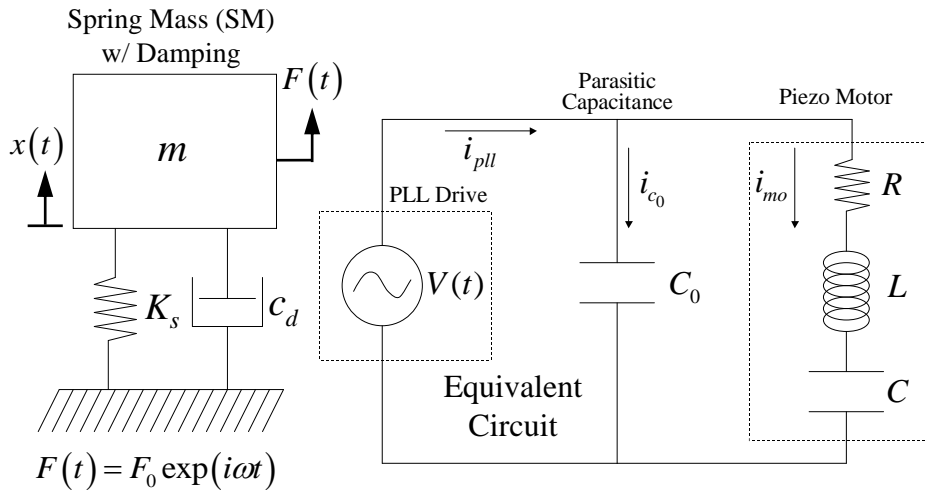
Typical Capillary Tool with Wire Compared to Sewing Needle

Motivation for the Research

- ❖ The displacement gain is the most important performance parameter for power ultrasonic transducers typically used for welding or cutting
 - ❖ It controls the proportional relationship between the displacement of the tool and the voltage or current input to the transducer, a key process parameter
- ❖ Due to aging effects of the PZT8 piezoceramics typically used in these transducers, and other variables such as gradual preload loss or tool clamp wear, the displacement gain can drift over time causing a shift in process and loss of machine-to-machine portability in mass production environments
- ❖ The “re-calibration” of the displacement gain usually involves a time consuming procedure of standardized controlled tests, and/or measurements using an expensive device such as a laser vibrometer
 - ❖ However, elementary engineering vibrations theory suggests that the displacement gain should be proportional to the static displacement (i.e., 0 Hz or DC) and the mechanical quality factor “ Q_m ” at resonance derived from a simple Bode plot, which is already familiar to most transducer designers
- ❖ This research investigates the methods for obtaining the mechanical quality factor from Bode plots (e.g., constant current or constant voltage sweeps), and ring-down techniques using logarithmic decrement, based on their predictability for determining the displacement gain
 - ❖ The investigation focuses solely on welding transducers for semiconductor wire bonding which employ common hard PZT8 piezoelectric materials
 - ❖ Several other metrics are investigated such as impedance, capacitance and electro-mechanical coupling factor
- ❖ The experimental and theoretical research methods include equivalent circuits, Bode plots, mechanical analogies and laser vibrometry

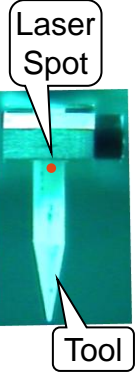
Definition of Q_m (Mechanical Quality Factor)

- ❖ Based on damped single DOF spring mass (SM) system
 - ❖ For forced response $F(t)$ at static x_s (F_0/K_s , $\omega = 0$) and resonant x_r ($\omega = \omega_r$) displacements: $Q_m = x_r/x_s$
 - ❖ For logarithmic decrement δ of free response ring-down of successive amplitudes: $Q_m = 1/2\zeta = \omega_r m/c_d$
- ❖ Based on energy balance of a damped vibrating system at resonance f_r
 - ❖ $Q_m = 2\pi \times$ energy stored in each cycle / energy dissipated in each cycle
 - ❖ $Q_m = 2\pi f_r \times$ energy stored / power loss
- ❖ Based on Bode plot near resonance at half-power -3dB bandwidth for transducer
 - ❖ $Q_m = f_r/\Delta f = f_r/(f_2 - f_1)$ (Also called Q_A based on IEEE standard 176-1987)
- ❖ Based on the admittance loop of equivalent RLC circuit of ultrasonic transducer
 - ❖ $Q_m = \omega_s P^2 X / P^2 R = \omega_s L / R = 1 / \omega_s C R$ (For reactance X , $Z_C = -1/j\omega C$, $Z_L = j\omega L$, at $\omega_s Z_C = -Z_L$, $\omega_s = 2\pi f_s$)
 - ❖ $Q_m = V_L / V_R = V_C / V_R$ (voltage drops at ω_s)

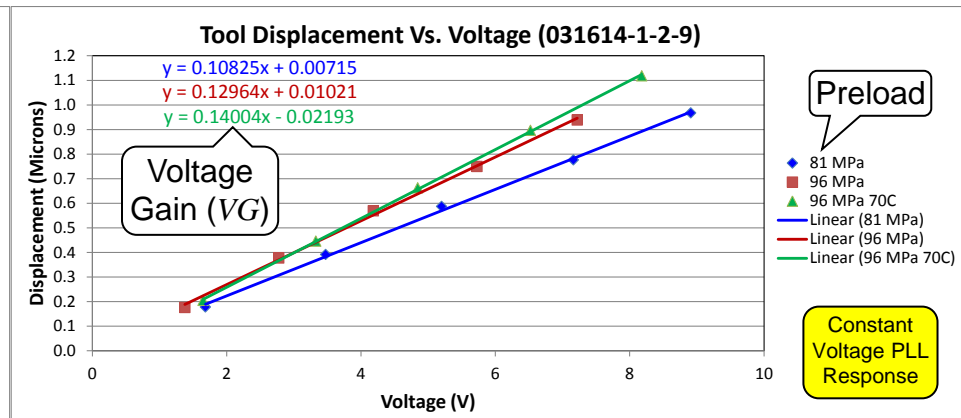
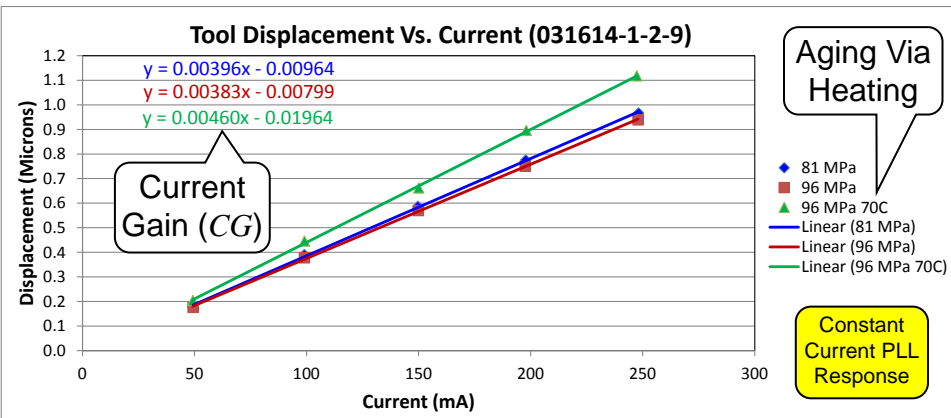


$$\omega_r = 2\pi f_r = \sqrt{\frac{K_s}{m}} \quad \delta = \frac{1}{n} \ln \left(\frac{x_i}{x_{i+n}} \right) \quad \zeta = \frac{\delta}{\sqrt{(2\pi)^2 + \delta^2}} = \frac{c_d}{2m\omega_r}$$

Definition of Displacement Gain

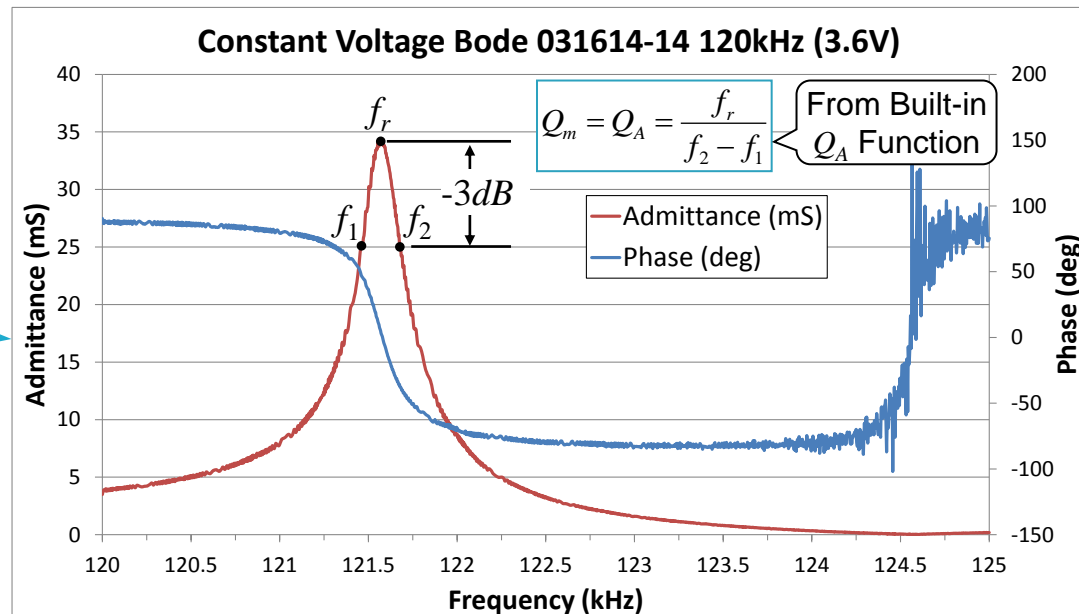
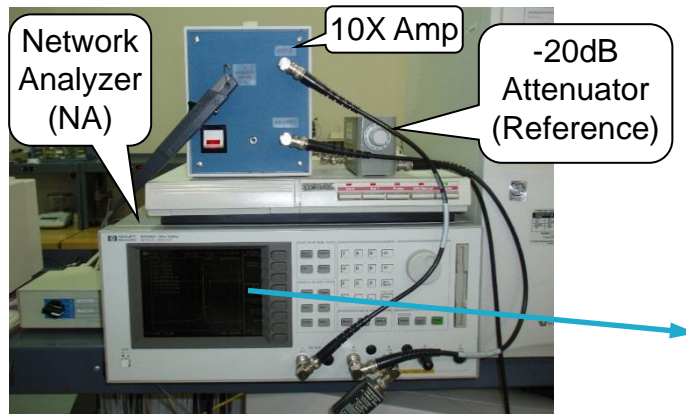


- ❖ The displacement gain is the linear relationship between the displacement of the tool (e.g., via laser vibrometer) and the voltage or current input to the transducer at the resonant operating mode
 - ❖ Expressed as either Voltage Gain (VG) or Current Gain (CG), these are the most important performance parameters for power ultrasonic transducers used in welding or cutting
- ❖ Most resonant phase-lock-loop (PLL) control systems work in either constant current (via CG) or constant voltage (via VG) mode (with C_0 compensation)
 - ❖ Constant current (CC) has the advantage of being insensitive to transducer impedance
 - ❖ Constant current mode maintains a constant tool displacement (i.e., velocity) during resonant operation resulting in more tool force being applied to the work as stiffness increases
 - ❖ Constant voltage (CV) mode maintains a constant force between the tool and the work during resonant operation, resulting in less tool displacement as stiffness increases
- ❖ Both the CG and VG can drift over time due to loss of preload, or aging effects (via heating, stress, time, etc.) of the piezoelectric stack requiring re-calibration



Methods for Measuring Q_m

- ❖ Constant voltage (CV) sweep Bode plot using network analyzer with 10X amplifier
 - ❖ Pros: The fastest and easiest way to measure Q_m using the built-in network analyzer (NA) equivalent circuit functions, or by measuring Q_m directly from admittance functions (a.k.a. Q_A via IEEE)
 - ❖ Cons: Current highly variable during sweep and suffers from “softening effects” at higher current/velocities causing non-symmetric admittance peak between f_1 and f_2 (w/ parasitic modes too)
 - ❖ Variables: Sweep voltage, sweep width and sweep time
- ❖ Ratio between quasi-static u_s (at 1kHz) and PLL resonant u_r displacements at constant voltage (can not drive high current for 1kHz off-resonance u_s)
 - ❖ Pros: The most consistent and repeatable measurements for Q_m
 - ❖ Cons: Difficult to implement in-process due to expensive equipment (e.g., laser vibrometer), and measurement must be made at constant voltage PLL making it sensitive to transducer impedance
 - ❖ Variables: Voltage level and PLL fire or burst time



From Built-in Equivalent Circuit Function

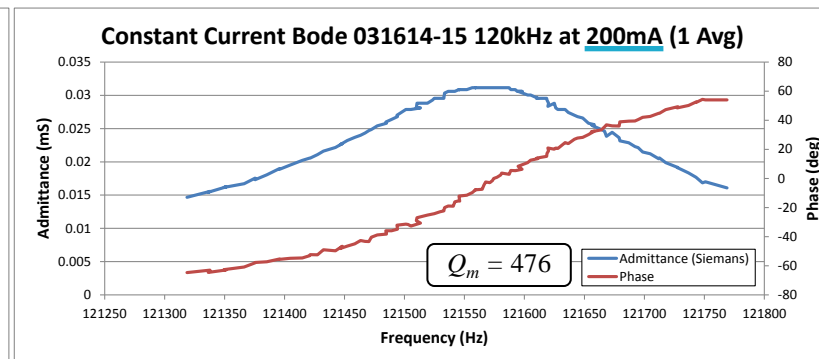
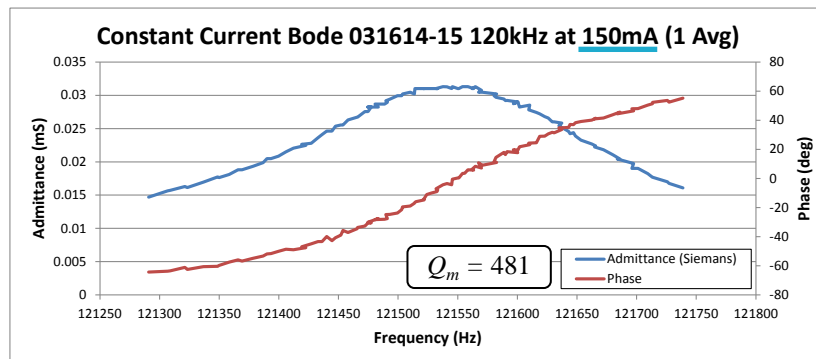
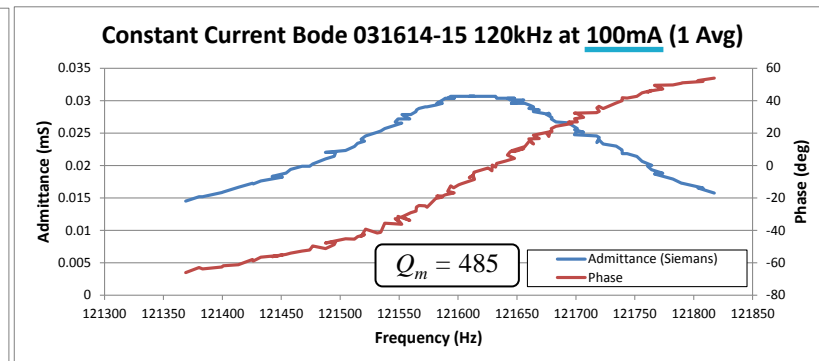
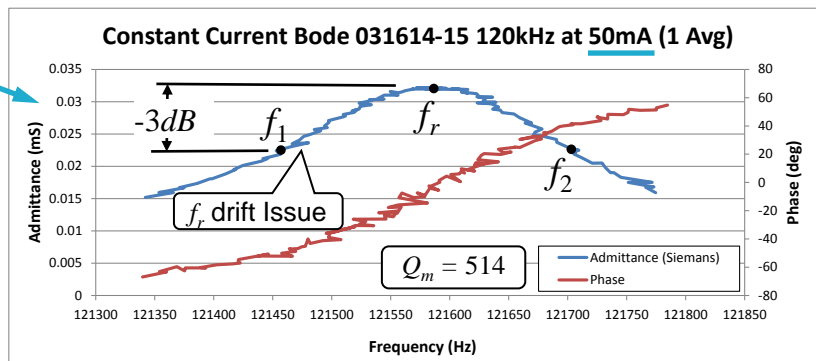
$$Q_m = \frac{\omega_s I^2 X}{I^2 R} = \frac{\omega_s L}{R} = \frac{1}{\omega_s C R}$$

Methods for Measuring Q_m (Con't)

- ❖ Constant current sweep Bode near f_r using phase offsets with PLL control system
 - ❖ Pros: Data taken at real operational conditions with actual current levels at f_r , f_1 and f_2
 - ❖ Cons: Data can be very noisy due to off-resonance heating at f_1 and f_2 (especially with higher impedance transducers) and random scatter from on/off PLL fires, which may require averaging from slight drifts in f_r . Can only be done in close vicinity of resonance f_r , since it will require higher voltage headroom for PLL at f_1 and f_2 for a given current. Motional current adjustment vs frequency may be required due parasitic loss through C_0 (usually small)
 - ❖ Variables: PLL fire or burst time, sweep width and current level. Re-establish f_r @ 0 phase after every sweep point plotting Δf_r with each phase offset (e.g., $f_r - f_1$ or $f_2 - f_r$), or use the same f_r @ 0 phase for all sweep points plotting actual frequency f at each phase offset (former used below)



Custom PLL Control System (Proprietary)

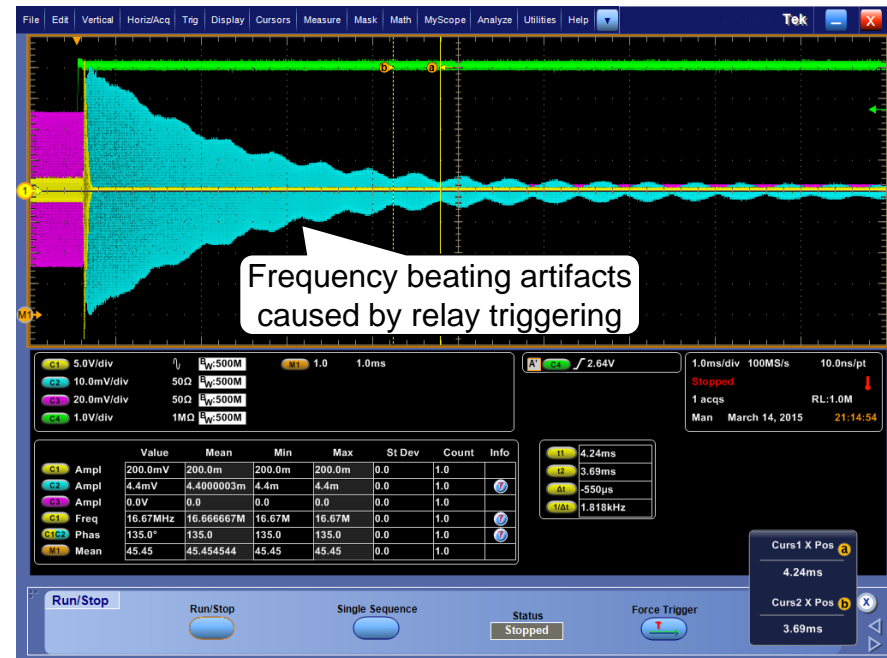
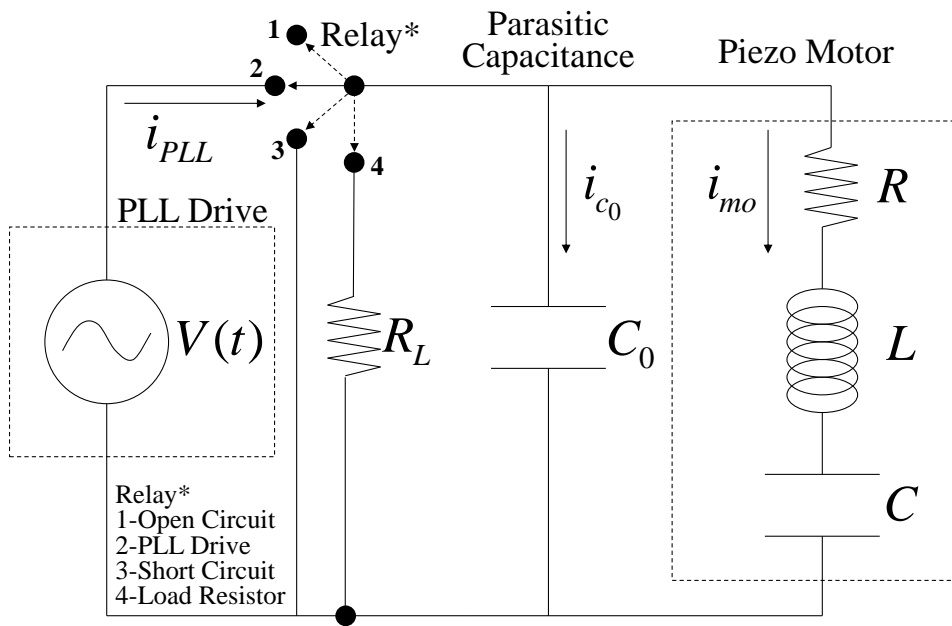


Constant Voltage (3.6V) Bode Reference for this Transducer

$Q_m = 524$

Methods for Measuring Q_m (Con't)

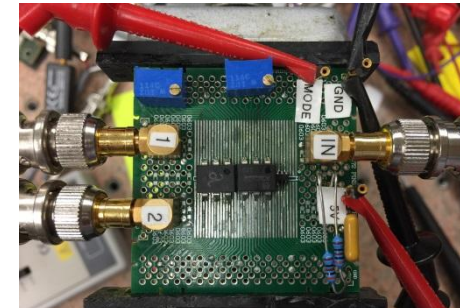
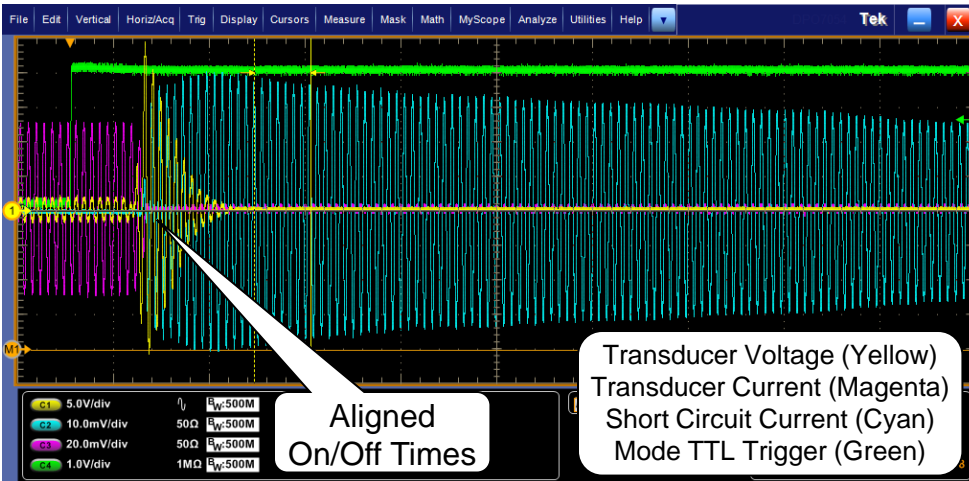
- ❖ Logarithmic decrement δ of ring-down after f_r resonant PLL drive via relay switch
 - ❖ Pros: Very flexible in-situ method that can be easily implemented at operating voltage or current, but also works with velocity via laser vibrometer. Can be implemented in three configurations, i.e., open circuit (OS), short circuit (SC) or load resistor (LR), allowing for different analytical models and analysis methods
 - ❖ Cons: Data can be noisy and difficult to analyze since Q_m is not constant during measurement as voltage or current decays in piezo stack (Q_m typically increases with decreasing current). Relay triggering can cause frequency beating type artifacts due to slow or misaligned open and close times, creating burst ring-down transitions of both open and closed circuit modes at the same time, and DC shifts
 - ❖ Variables: PLL current or voltage level, PLL time, relay trigger and ring-down range (e.g. I_{start} , I_{end})



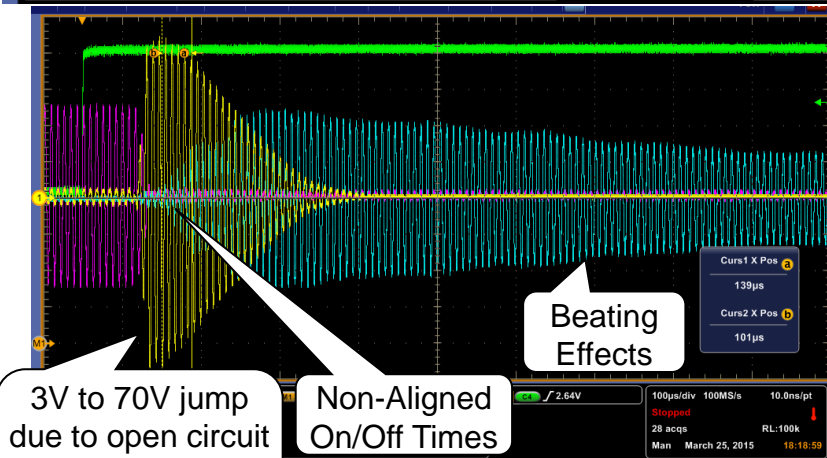
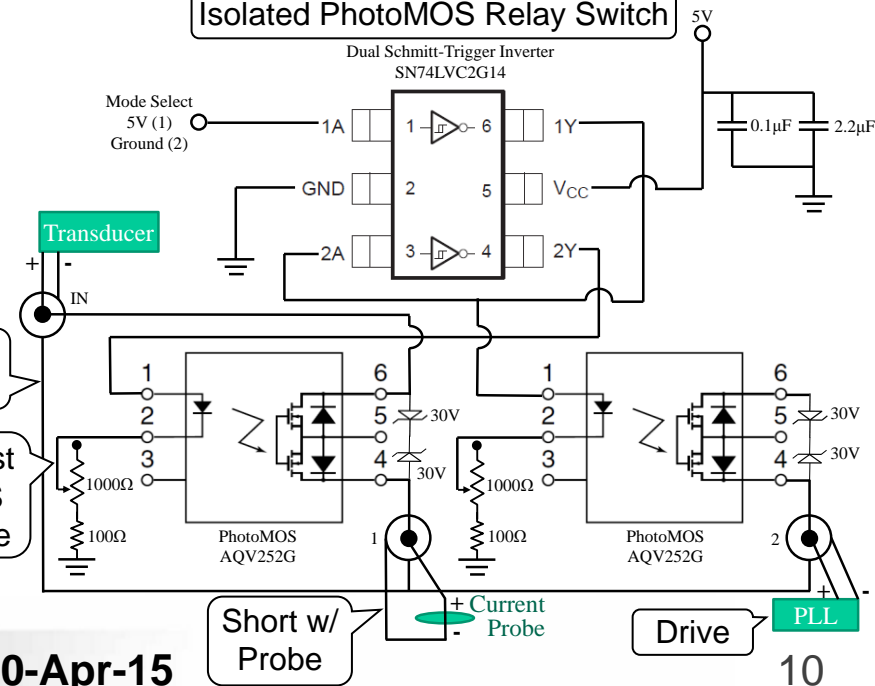
Methods for Measuring Q_m (Con't)

Details: Logarithmic decrement δ in short circuit using replay switch & current probe

- ❖ Relay Ports: Transducer \rightarrow IN, PLL \rightarrow 2 and Short to Isolated Ground with Current Probe \rightarrow 1
- ❖ Frequency generator TTL input to Mode Select at 0.1Hz frequency (5V-Port 1, Ground-Port 2)
- ❖ Potentiometer (1000 Ω) for each PhotoMOS adjusted to align PLL turn-off time with SC turn-on time
- ❖ PLL current set to 100mA with SC ring-down recorded over 70-50mA range (i.e., $I_{start} - I_{end}$)

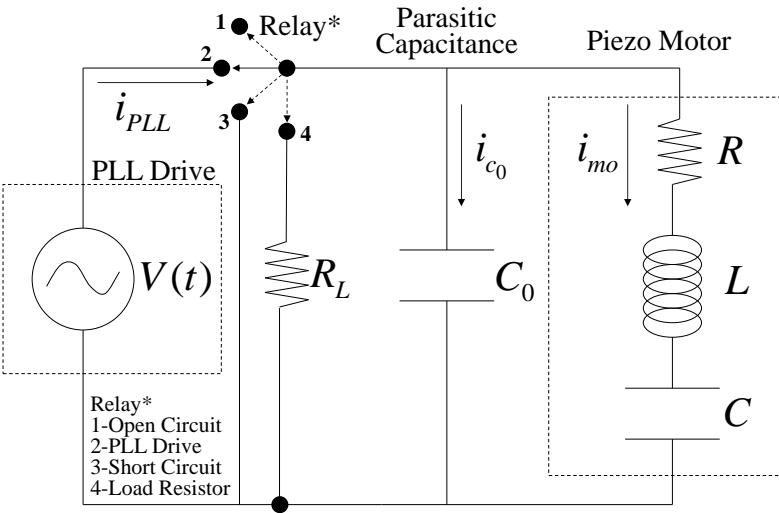


Isolated PhotoMOS Relay Switch



Equivalent Circuit Analysis for δ

- ❖ The logarithmic decrement δ can be implemented in three modes (OC, SC, LR)
 - ❖ For resonant PLL drive $i_{PLL} \approx i_{mo}$. For open circuit (OC) ring down $i_{co} = -i_{mo}$, so only voltage can be measured for predicting Q_m at parallel mode f_p anti-resonance. For short circuit (SC) ring down $i_{co} = 0$, so only current can be measured for predicting Q_m at series mode f_s resonance. For load resistor (LR) ring down, both the voltage and current can be measured at ring-down between f_s and f_p
 - ❖ For the PLL drive (2-Relay) the circuit resonates in the series mode ω_s when the reactance from the L and C cancel, so we can assume $i_{PLL} \approx i_{mo} = i$



Apply Kirchoff's law to outer loop and take d/dt

$$L \frac{d^2 i}{dt^2} + R \frac{di}{dt} + \frac{1}{C_0} i = \frac{d}{dt} V(t) \quad \text{①} \quad V(t) = V_0 \sin(\omega_{PPL} t)$$

The steady-state particular solution is given as

$$i(t) = \frac{V_0 C}{\sqrt{(1-r^2)^2 + (2\zeta r)^2}} \sin(\omega_{PPL} t - \psi) \quad \text{②}$$

$$r = \frac{\omega_{PPL}}{\omega_s} \quad \omega_s = \frac{1}{\sqrt{LC}} \quad \psi = \text{atan}\left(\frac{2\zeta r}{1-r^2}\right) \quad \zeta = \frac{R}{2L\omega_s}$$

- ❖ For the SC ring down (3-Relay), we solve the homogenous solution of ① with the initial conditions from the ②

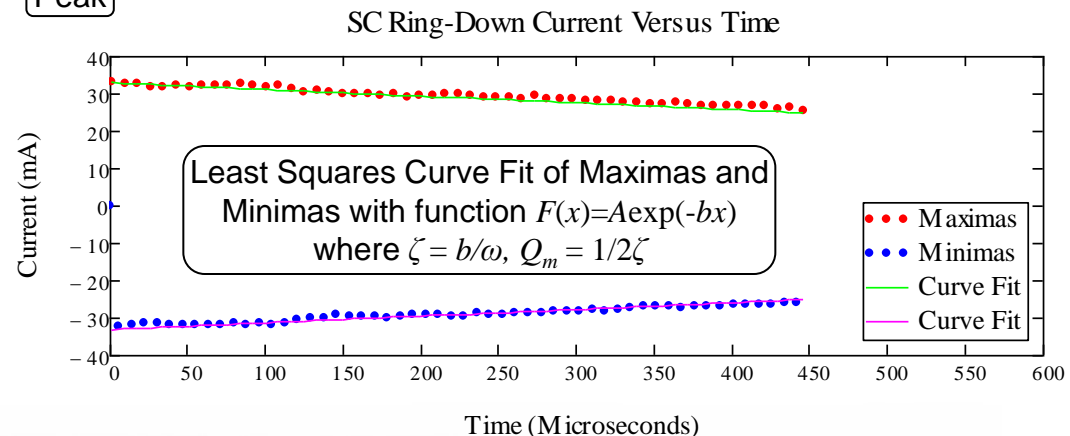
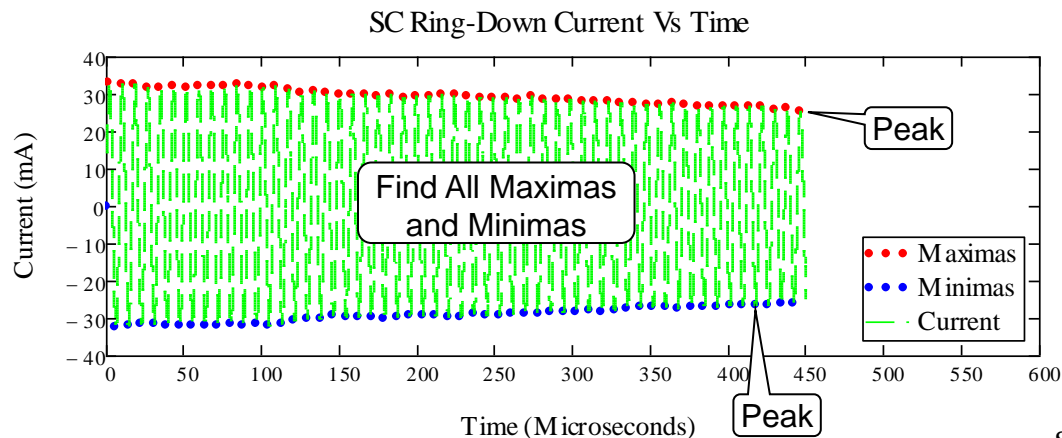
From initial conditions at $t = 0$

$$i(t) = \exp(-\zeta \omega t) (A \cos(\omega_d t) + B \sin(\omega_d t)) \quad \text{③} \quad \omega_d = \sqrt{1-\zeta^2} \omega_s \quad A = i(0) \quad -\zeta \omega A + B \omega_d = \left. \frac{d}{dt} i(t) \right|_{t=0}$$

- ❖ For OC ring down (1-Relay), the circuit resonates in the parallel mode ω_p with initial conditions from ②, where $i_{mo} = -i_{co} = i$. Solution is given by ③ with $\omega_d = \sqrt{1-\zeta^2} \omega_p$ $\omega_p = \sqrt{\frac{C_0 + C}{LC_0 C}}$ $\zeta = \frac{R}{2L\omega_p}$

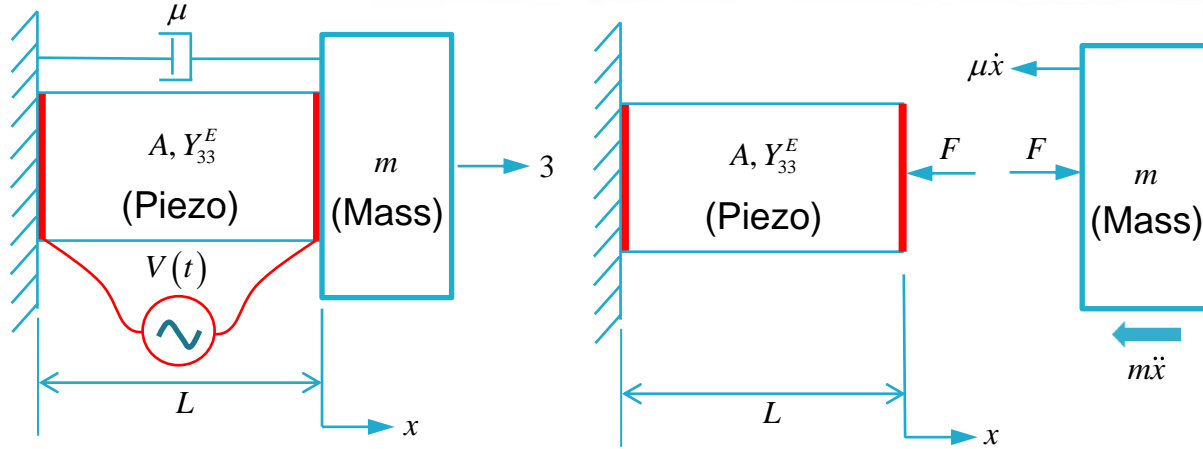
Numerical Data Analysis for δ

- ❖ Logarithmic decrement analysis performed in Mathcad (*Mathcad function*)
 - ❖ Save waveform data from each channel from Tektronix scope into Mathcad format
 - ❖ Plot data to truncate for the desired ring-down range of I_{start} and I_{end} (e.g., 70 to 50 mA)
 - ❖ Perform data smoothing (*ksmooth*) and apply cubic spline approximation (*cspline*, *interp*)
 - ❖ Find all actual minimas and maximas by iterating through data to separate out local ones near peaks
 - ❖ Use least squares curve fit approximation of peaks with function $F(x)=A\exp(-bx)$ (*genfit*) to determine ζ



Displacement Gain Vs. Q_m Derivation

Example Derivation ($m \gg$ mass of piezo rod, $L < \lambda/4$)



Mechanical Eq of Motion

$$\sum F = 0 \rightarrow F(t) = m\ddot{x}(t) + \mu\dot{x}(t) \quad \text{①}$$

Piezo Equations

Stress $S = s^E \cdot T + d^t \cdot E$ ②

Strain Compliance $\frac{\text{Charge}}{\text{Force}}$ or $\frac{m}{V}$

Charge (Q) Area (A) $D = d \cdot T + \epsilon^T \cdot E$ ③

Permittivity (F/m) Electric Field (V/m)

Apply Eq ② $\rightarrow \frac{x(t)}{L} = \frac{-F(t)}{AY_{33}^E} + d_{33} \frac{V(t)}{L} \rightarrow F(t) = \frac{AY_{33}^E}{L} (d_{33}V(t) - x(t))$ ④ \rightarrow Sub Eq ① $\rightarrow \ddot{x}(t) + \frac{\mu}{m}\dot{x}(t) + \frac{AY_{33}^E}{mL}x(t) = \frac{AY_{33}^E}{mL}d_{33}V(t)$ ⑤

Apply Eq ③ $\rightarrow \frac{Q(t)}{A} = d_{33} \frac{-F(t)}{A} + \epsilon_{33}^T \frac{V(t)}{L} \rightarrow I(t) = \frac{dQ(t)}{dt}$ Sub assumed solutions into ⑤, eliminate $\exp(i\omega t)$ & sub $K_s = \frac{AY_{33}^E}{L}$

Assume solutions in form $X_0 \exp(i\omega t)$

Sub Eq ④ with $I(t) = I_0 \exp(i\omega t) \rightarrow I_0 = \left[\frac{A\epsilon_{33}^T}{L} - d_{33}^2 \frac{AY_{33}^E}{L} \right] i\omega V_0 + d_{33} \frac{AY_{33}^E}{L} i\omega x_0$ $-x_0\omega^2 + \frac{\mu}{m}x_0i\omega + \frac{AY_{33}^E}{mL}x_0 = \frac{AY_{33}^E}{mL}d_{33}V_0 \rightarrow x_0 = \frac{K_s}{\left(\frac{K_s}{m} - \omega^2 + \frac{\mu}{m}i\omega \right)} d_{33}V_0$ ⑥

Sub for K_s with $C_0 = \frac{A\epsilon_{33}^T}{L} = \frac{A\epsilon_r^T}{L}\epsilon_0 \rightarrow I_0 = [C_0 - d_{33}^2 K_s] i\omega V_0 + d_{33} K_s i\omega x_0$

Sub $\omega_0^2 = \frac{K_s}{m}$ $\zeta = \frac{\mu}{2m\omega_0} = \frac{1}{2Q_m}$ in ⑥ and solve Re part

Sub Eq ⑦ & ③, solve for current gain (CG) at resonance $\omega \rightarrow \omega_0$

$$CG^{\omega \rightarrow \omega_0} = \frac{\text{Re}\{x(t)^{\omega \rightarrow \omega_0}\}}{\text{Re}\{I(t)^{\omega \rightarrow \omega_0}\}} = \frac{|x_0^{\omega \rightarrow \omega_0}|}{|I_0^{\omega \rightarrow \omega_0}|} = \frac{Q_m d_{33}}{C_0 \omega_0 + [Q_m - 1] K_s \omega_0^2} = \frac{Q_m d_{33}}{C_0 \omega_0 + [Q_m - 1] \omega_0 k_{33}^2 C_0}$$

$$x(t) = \text{Re}\{x_0 \exp(i\omega t)\} = \frac{x_0^{\omega \rightarrow 0}}{|a + bi|} \text{Re}\{\exp(i\omega t)\} \quad x_0^{\omega \rightarrow 0} = d_{33}V_0$$

(Static x)

Voltage gain (VG) is defined from $x_0^{\omega \rightarrow \omega_0} = Q_m x_0^{\omega \rightarrow 0} = (Q_m d_{33})V_0 = (VG)V_0$ ⑦

For transducers, $k_e = k_{33}$ and $d_e = d_{33}$

$$CG = \frac{Q_m d_e}{C_0 \omega_0 + [Q_m - 1] \omega_0 k_e^2 C_0} \quad VG = Q_m d_e$$

$$d_e = \frac{x_0^{\omega \rightarrow 0}}{V_0} = \frac{u_s}{V_0} \quad k_e = \sqrt{1 - \frac{f_s^2}{f_p^2}}$$

E-mech Coupling Definition (k)

$$k^2 = \frac{\text{Energy}_{\text{mech}}^{\text{stored}}}{\text{Energy}_{\text{elec}}^{\text{in}}} = \frac{\frac{1}{2} k_x x^2}{\frac{1}{2} CV^2} = \frac{\frac{1}{2} \left(\frac{AY^E}{L} \right) (dV)^2}{\frac{1}{2} \left(\frac{A\epsilon_r^T}{L} \right) V^2} = \frac{Y^E d^2}{\epsilon_r^T}$$

$$k_{33}^2 = \frac{Y_{33}^E d_{33}^2}{\epsilon_{r33}^T} = \frac{\left(\frac{AY_{33}^E}{L} \right) d_{33}^2}{\left(\frac{A\epsilon_{r33}^T}{L} \right)} = \frac{K_s^E d_{33}^2}{C_0} = \frac{d_{33}^2}{C_0 C}$$

Experimental Results

Summary of experimental data for 10 random transducers (amplitudes p-to-p)

Transducer Serial #	LCR Meter (1kHz)		NA CV Bode w/ 10X Amp				PLL CC Bode		Static Displ. Test			Resonant Displacement Test				SC Ring-Down Test			Displacement Gains & Power		
	C_0	DF	f_r (Hz)	$Z(\Omega)$	k_e	Q_m	I_{pll} (mA)	Q_m	V_s (V)	f (Hz)	u_s (μ m)	V_r (V)	I_r (mA)	u_r (μ m)	Q_m	I_{start} (mA)	I_{end} (mA)	Q_m	μ m/mA	μ m/V	μ m ² /W
031614	1721	0.004	121569	29	0.2167	524	50	514	100	1000	0.036	1.518	50	0.215	396	70	50	621	0.00472	0.16046	0.73683
SF19315L	1710	0.004	120963	19	0.2107	836	50	806	100	1000	0.035	0.953	50	0.223	668	70	50	1371	0.00502	0.23987	1.18574
SF19319L	1705	0.004	122372	16	0.2094	943	50	1121	100	1000	0.034	0.750	50	0.232	904	70	50	1413	0.00499	0.28288	1.42318
SF19331L	1691	0.004	121591	20	0.2063	802	50	894	100	1000	0.035	1.038	50	0.220	605	70	50	787	0.00487	0.21955	1.05099
SF19327L	1692	0.004	121378	20	0.2071	831	50	906	100	1000	0.035	1.012	50	0.230	649	70	50	569	0.00482	0.21088	1.01881
SF19312L	1677	0.004	121206	19	0.2094	934	50	879	100	1000	0.035	0.948	50	0.221	666	70	50	908	0.00479	0.24176	1.14117
SF20753L	1635	0.003	122725	48	0.1817	460	50	418	100	1000	0.029	2.500	50	0.262	366	70	50	537	0.00562	0.10794	0.59916
SF23402L	1561	0.003	121816	35	0.1819	653	50	495	100	1000	0.029	1.849	50	0.279	526	70	50	552	0.00592	0.14566	0.85943
SF22980L	1551	0.003	120878	36	0.1877	629	50	573	100	1000	0.030	1.875	50	0.280	494	70	50	731	0.00597	0.15860	0.93089
SF20752L	1637	0.003	123172	26	0.1801	804	50	495	100	1000	0.029	1.349	50	0.247	640	70	50	581	0.00559	0.16758	0.93418

Summary of predictions for Current Gain (CG) and Voltage Gain (VG)

- The static displacement u_s is very consistent across all transducers, so the measurement for d_e only needs to be done infrequently after transducer is placed in service (or just once before)
- Alternately, the effective E-mech coupling k_e from NA CV Bode is also an excellent predictor for u_s

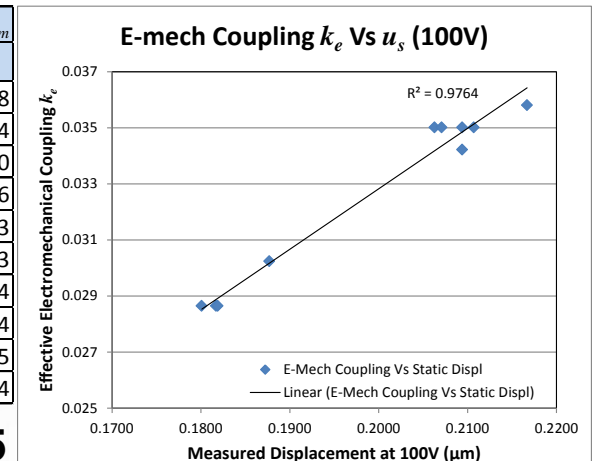
$$CG = \frac{Q_m d_e}{C_0 \omega_0 + [Q_m - 1] \omega_0 k_e^2 C_0}$$

$$VG = Q_m d_e$$

Where

$$d_e = \frac{u_s}{V_s} \quad k_e = \sqrt{1 - \frac{f_s^2}{f_p^2}}$$

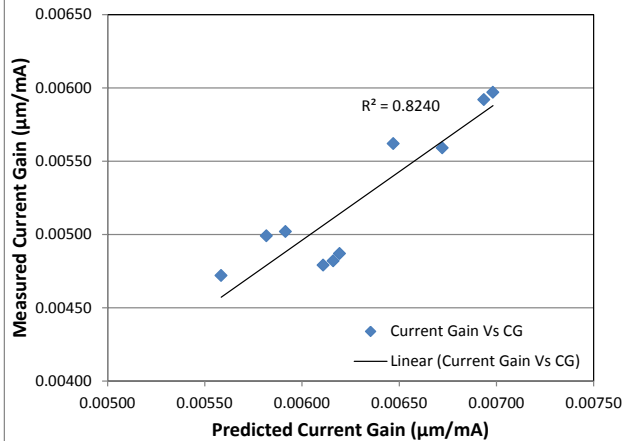
Transducer Serial #	Measured Displacement Gains		NA CV Bode Q_m		PLL CC Bode Q_m		$u_r/u_s Q_m$		SC Ring-Down Q_m	
	μ m/mA (CG)	μ m/V (VG)	CG	VG	CG	VG	CG	VG	CG	VG
031614	0.00472	0.16046	0.00558	0.18764	0.00558	0.18406	0.00552	0.14163	0.00562	0.22238
SF19315L	0.00502	0.23987	0.00592	0.29262	0.00591	0.28221	0.00588	0.23400	0.00597	0.48004
SF19319L	0.00499	0.28288	0.00582	0.32254	0.00584	0.38359	0.00581	0.30933	0.00586	0.48350
SF19331L	0.00487	0.21955	0.00619	0.28072	0.00621	0.31303	0.00614	0.21195	0.00619	0.27556
SF19327L	0.00482	0.21088	0.00616	0.29099	0.00617	0.31723	0.00612	0.22731	0.00609	0.19923
SF19312L	0.00479	0.24176	0.00611	0.32715	0.00610	0.30777	0.00605	0.23324	0.00611	0.31793
SF20753L	0.00562	0.10794	0.00647	0.13175	0.00643	0.11975	0.00637	0.10480	0.00653	0.15384
SF23402L	0.00592	0.14566	0.00694	0.18719	0.00684	0.14181	0.00687	0.15073	0.00688	0.15814
SF22980L	0.00597	0.15860	0.00698	0.19018	0.00695	0.17327	0.00690	0.14951	0.00702	0.22105
SF20752L	0.00559	0.16758	0.00672	0.23025	0.00658	0.14181	0.00666	0.18340	0.00663	0.16644



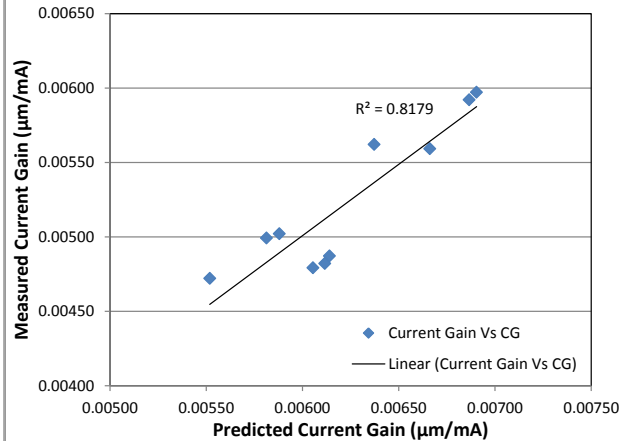
Experimental Results (Con't)

- ❖ Regression analysis of measured data vs. predicted gain data for various Q_m methods on 10 random transducers. What is most important is the relative change or slope, not the absolute value

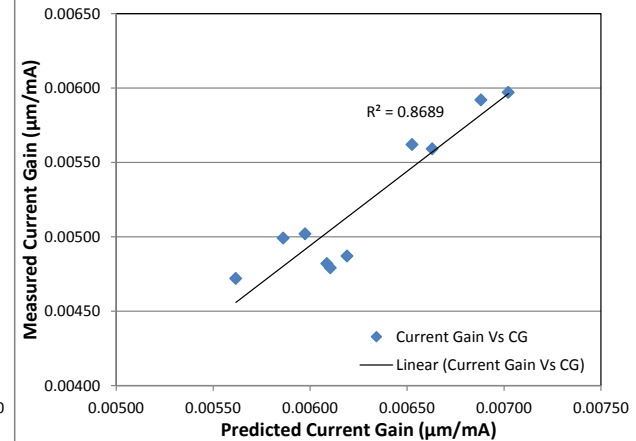
Current Gain Vs CG (NA CV Bode Q_m)



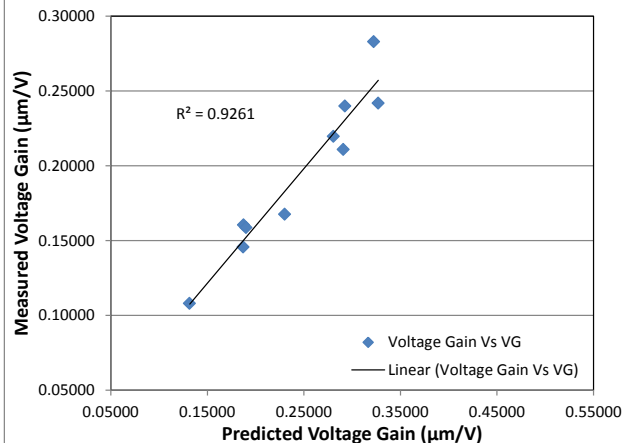
Current Gain Vs CG (u_r/u_s Q_m)



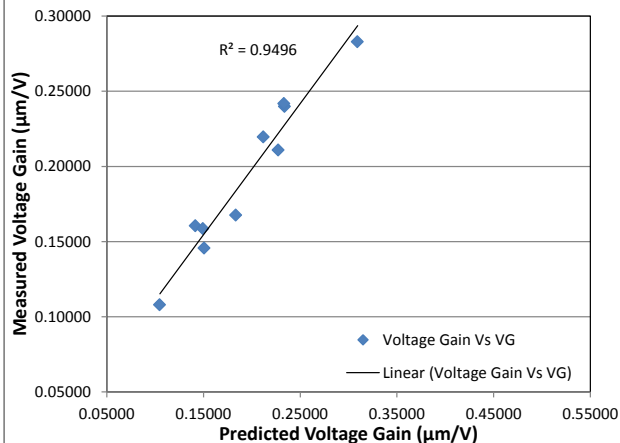
Current Gain Vs CG (SC Ring-Dwn Q_m)



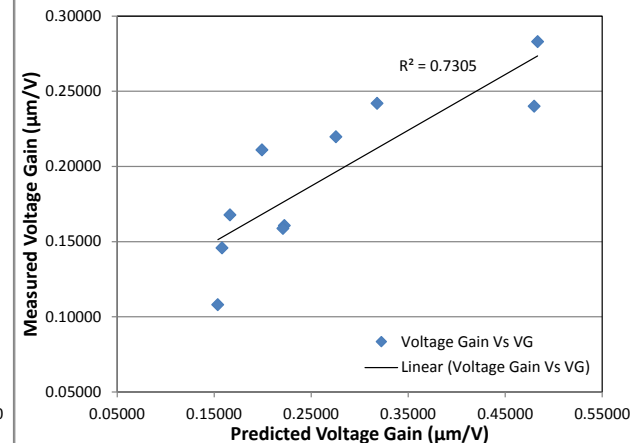
Voltage Gain Vs VG (NA CV Bode Q_m)



Voltage Gain Vs VG (u_r/u_s Q_m)

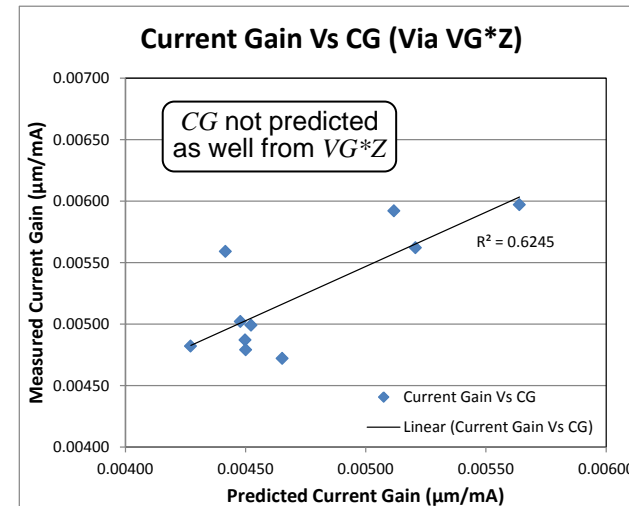
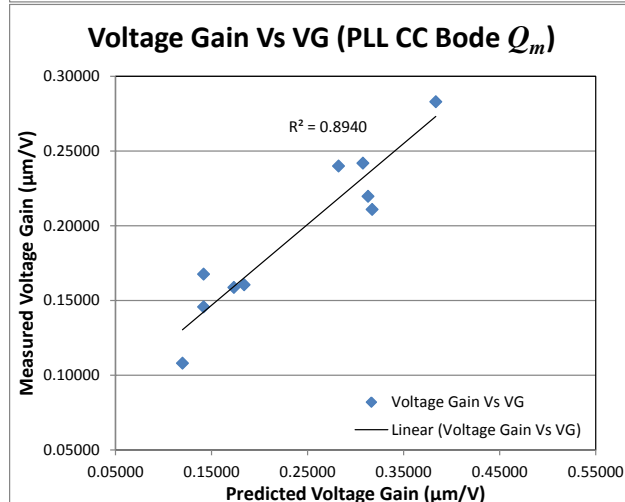
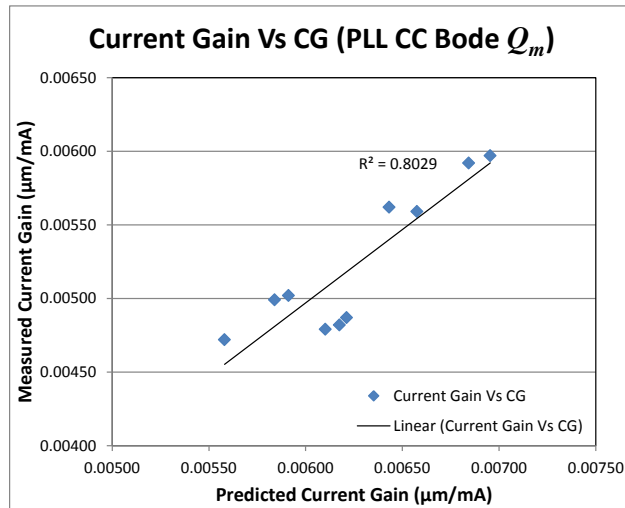


Voltage Gain Vs VG (SC Ring-Dwn Q_m)



Experimental Results (Con't)

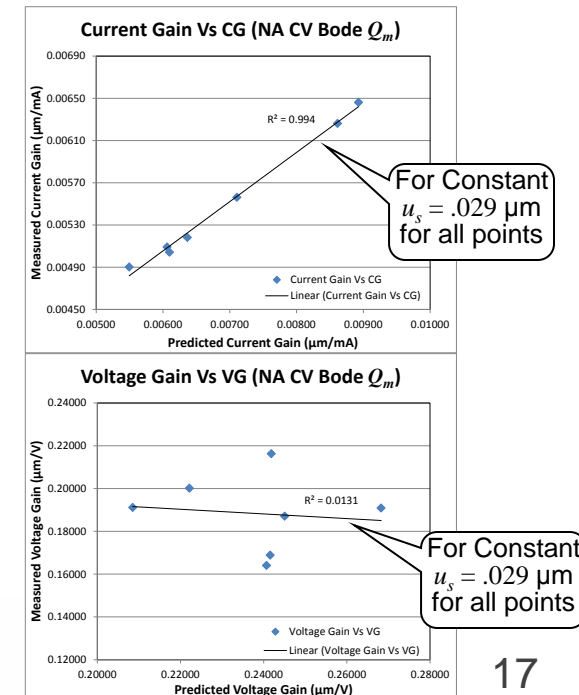
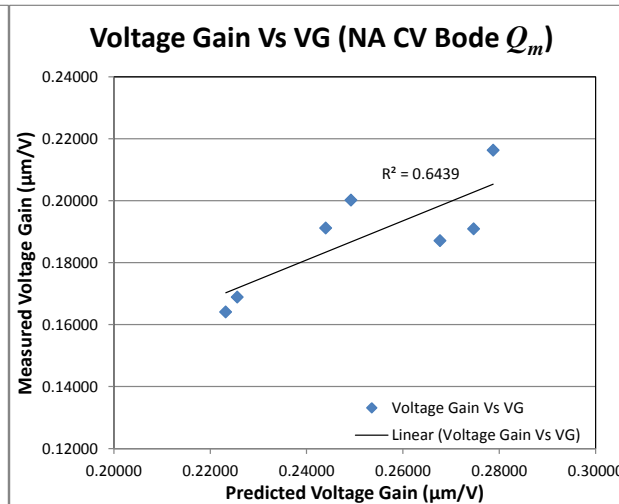
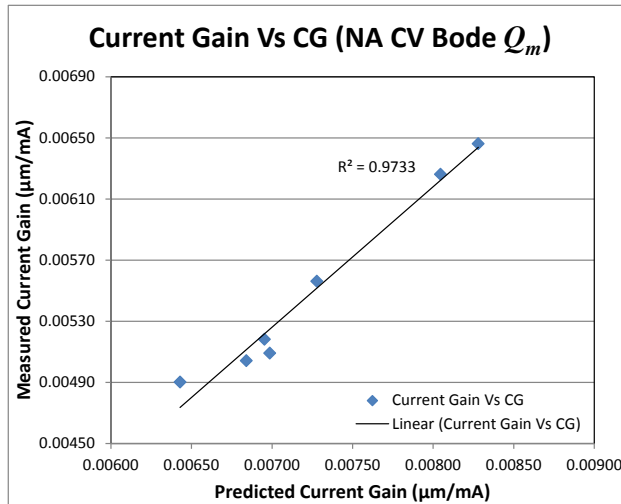
- ❖ Regression analysis of measured data vs. predicted gain data for various Q_m methods on 10 random transducers. What is most important is the relative change or slope, not the absolute value



Experimental Results (Con't)

- ❖ Predicted gain data for one transducer subjected to multiple heat-treatments
 - ❖ Old data from previous study where only Q_m from NA CV Bode plot was available (no u_s data either)
 - ❖ Static displacement u_s was estimated based on E-mech coupling k_e from Bode plots $u_s^{X^\circ C} = \frac{k_e^{X^\circ C}}{k_e^{70^\circ C}} u_s^{70^\circ C}$

Transducer Serial #	Heat Treatment (°C)	LCR Meter (1kHz)		NA CV Bode w/ 10X Amp				Static Displ. Test			Displacement Gains		NA CV Bode Q_m	
		C_0	DF	f_r (Hz)	Z (Ω)	k_e	Q_m	V_s (V)	f (Hz)	u_s (μm)	$\mu m/mA$	$\mu m/V$	CG	VG
SF16655L-2	70	1576	0.004	122575	20	0.1956	834	100	1000	0.033	0.00509	0.21625	0.00699	0.27874
SF16655L-3	75	1682	0.005	122475	23	0.1986	719	100	1000	0.034	0.00490	0.19116	0.00643	0.24399
SF16655L-4	80	1645	0.004	122675	25	0.1904	766	100	1000	0.033	0.00504	0.20016	0.00684	0.24921
SF16655L-5	85	1664	0.004	122700	25	0.1854	845	100	1000	0.032	0.00518	0.18705	0.00695	0.26769
SF16655L-8	100	1690	0.003	122950	27	0.1738	925	100	1000	0.030	0.00556	0.19088	0.00728	0.27470
SF16655L-10	110	1653	0.003	123275	30	0.1585	833	100	1000	0.027	0.00626	0.16889	0.00805	0.22560
SF16655L-11	110	1615	0.004	123350	31	0.1574	830	100	1000	0.027	0.00646	0.16404	0.00828	0.22323



Conclusions

- ❖ All four methods (i.e., NA/PLL Bode, u_r/u_s & δ) presented for Q_m provided good agreement to experimental results for predicting relative change in VG and CG
 - ❖ Since the Q_m can vary greatly with amplitude of vibration, velocity, current, voltage and temperature, only the relative change is important for prediction of VG and CG
 - ❖ This wire bonding transducer application may not accentuate the different Q_m methods, since it is fairly low duty cycle (20%), and is driven at the lower end of power capability for PZT8 (for stability)
- ❖ The VG is mostly correlated to Q_m , but the CG is mostly influenced by k_e (not Q_m)
- ❖ The u_r/u_s method is most accurate for VG at any power level, but is difficult to implement in-process due to expensive in-situ equipment such as vibrometer
- ❖ The NA CV Bode method is good predictor of CG and VG at low power, but has known issues at higher amplitudes due to softening effects causing distortion
 - ❖ Excellent results were still seen with the NA CV Bode method for predicting CG changes after multiple heat-treatments, but the VG is less correlated with just estimates for u_s based on k_e
- ❖ The PLL CC Bode method is a good predictor of CG and VG at all power levels, but has f_r drift issues due to off-resonance heating (averaging helps)
- ❖ The ring-down δ method is a good predictor for CG , and can also be used at any power level
 - ❖ It is also the easiest to implement in-process under actual bonding conditions with k_e from CV Bode
 - ❖ However, it was the least accurate for VG due to random variation in the Q_m measurement caused by beating effects from relay switch (still working on improving this)
- ❖ The static displacement u_s was found to be highly correlated to k_e
 - ❖ This greatly simplifies the requirements for measuring u_s over time for VG prediction
- ❖ The CG is not predicted well by $VG*Z$, which is an indication of higher order effects from the E-mech coupling k_e

References

- ❖ K. F. Graff, Wave Motion in Elastic Solids. New York, NY: Dover Publications, 1991.
- ❖ C. H. Sherman and J. L. Butler, Transducers and Arrays for Underwater Sound. New York, NY: Springer Science, 2007.
- ❖ D. Stansfield, Underwater Electroacoustic Transducers. Los Altos, CA: Peninsula Publishing, 1991.
- ❖ K. Uchino and J. R. Giniewicz, Micromechatronics. New York, NY: Marcel Dekker, 2003.
- ❖ R. S. Woollett, "Transducer Comparison Methods Based on the Electromechanical Coupling-Coefficient Concept," 1957 IRE National Convention, p. 23-27, IEEE Xplore.
- ❖ D. V. Hutton, Applied Mechanical Vibrations. New York, NY: McGraw-Hill, 1981.
- ❖ A. Erturk and D. J. Inman, Piezoelectric Energy Harvesting. UK: John Wiley & Sons, 2011.
- ❖ D. Ensminger, F.B. Stulen, Ultrasonics: Data, Equations, and Their Practical Uses. Boca Raton, FL: CRC Press, 2009.
- ❖ M. Umeda, K. Nakamura, S. Takahashi and S. Ueha, "An Analysis of Jumping and Dropping Phenomena of Piezoelectric Transducers using the Electrical Equivalent Circuit Constants at High Vibration Amplitude Levels," Japanese Journal of Applied Physics Vol. 39 (2000) pp. 5623-5628.
- ❖ M. Umeda, K. Nakamura and S. Ueha, "The Measurement of High-Power Characteristics for a Piezoelectric Transducer Based on the Electrical Transient," Japanese Journal of Applied Physics Vol. 37 (1998) pp. 5322-5325.
- ❖ S. O. Ural, S. Tuncdemir, Y. Zhuang and K. Uchino, "Development of a High Power Piezoelectric Characterization System and Its Application for Resonance/Antiresonance Mode Characterization," Japanese Journal of Applied Physics 48 (2009) 056509.
- ❖ K. Uchino, Y. Zhuang, S. O. Ural, "Loss Determination Methodology for a Piezoelectric Ceramic: New Phenomenological Theory and Experimental Proposals," Journal of Advanced Dielectrics, Vol. 1 No. 1 (2011) pp. 17-31.
- ❖ W. A. T. Mohammed, J. O. Dennis and M. K. A. M. Ahmed, "Damping Effect on The Q-factor Value of A MEMS Magnetic Field Sensor," ICIEE 2012 Proceedings.
- ❖ H. N. Shekhani and K. Uchino, "Evaluation of the Mechanical Quality Factor Under High Power Conditions in Piezoelectric Ceramics from Electrical Power," Journal of the European Ceramic Society Vol 35 (2105) pp. 541-544.
- ❖ K. Chang and M. Ouyang, "Open-Circuit Test of a PZT Vibrator and Its Applications," Ultrasonics Vol 41 (2003) 15-23

References

- ❖ O. B. Wilson, Introduction to Theory and Design of Sonar Transducers. Los Altos, CA: Peninsula Publishing, 1991.
- ❖ K. Uchino, Ferroelectric Devices. New York, NY: Marcel Dekker, 2010.
- ❖ K. Nakamura (Editor), Ultrasonic Transducers: Materials and Design for Sensors, Actuators and Medical Applications. Philadelphia, PA: Woodhead Publishing, 2012.
- ❖ J. R. Frederick, Ultrasonic Engineering. New York, NY: John Wiley & Sons, 1965.
- ❖ A. Arnau, Piezoelectric Transducers and Applications. New York, NY: Springer-Verlag, 2004.
- ❖ J. W. Waanders, Piezoelectric Ceramics: Properties and Applications. Eindhoven, Netherlands: N. V. Philips' Gloeilampenfabrieken, 1991.

- ❖ D. A. DeAngelis and G. W. Schulze, "Performance of PIN-PMN-PT Single Crystal Piezoelectric Versus PZT8 Piezoceramic Materials in Ultrasonic Transducers," 2014 UIA Symposium Proceedings, Physics Procedia.
- ❖ D. A. DeAngelis and G. W. Schulze, "Optimizing Piezoelectric Stack Preload Bolts in Ultrasonic Transducers," 2013 UIA Symposium Proceedings, Physics Procedia.
- ❖ D. A. DeAngelis and G. W. Schulze, "The Effects of Piezoelectric Ceramic Dissipation Factor on the Performance of Ultrasonic Transducers," 2012 UIA Symposium Proceedings, Physics Procedia.
- ❖ D. A. DeAngelis and G. W. Schulze, "Advanced Bode Plot Techniques for Ultrasonic Transducers," 2011 UIA Symposium Proceedings, Physics Procedia.
- ❖ D. A. DeAngelis and G. W. Schulze, "Optimizing Piezoelectric Ceramic Thickness in Ultrasonic Transducers," 2010 UIA Symposium Proceedings, IEEE XPlore.
- ❖ D. A. DeAngelis and G. W. Schulze, "Optimizing Piezoelectric Crystal Preload in Ultrasonic Transducers," 2009 UIA Symposium Proceedings, IEEE XPlore.
- ❖ D. A. DeAngelis and D. C. Schalcosky, "The Effect of PZT8 Piezoelectric Crystal Aging on Mechanical and Electrical Resonances in Ultrasonic Transducers," 2006 IEEE Ultrasonics Symposium, Session P2O-10.

Questions?